Coalescence in the 1D Cahn–Hilliard model

2004 J. Phys. A: Math. Gen. 37 6929

(http://iopscience.iop.org/0305-4470/37/27/005)

INSTITUTE OF PHYSICS PUBLISHING JOURNAL OF PHYSICS A: MATHEMATICAL AND GENERAL

J. Phys. A: Math. Gen. **37** (2004) 6929–6941 PII: S0305-4470(04)73397-1

Coalescence in the 1D Cahn–Hilliard model

Simon Villain-Guillot

Centre de Physique Moléculaire Optique et Hertzienne, Université Bordeaux I, 33406 Talence Cedex, France

E-mail: s.villain@cpmoh.u-bordeaux1.fr

Received 11 December 2003, in final form 7 April 2004
Published 22 June 2004
Online at stacks.iop.org/JPhysA/37/6929
doi:10.1088/0305-4470/37/27/005

Abstract

We present an approximate analytical solution of the Cahn–Hilliard equation describing the coalescence during a first-order phase transition. We have identified all the intermediate profiles, stationary solutions of the noiseless Cahn–Hilliard equation. Using properties of the soliton lattices, periodic solutions of the Ginzburg–Landau equation, we have constructed a family of ansätze describing continuously the process of destabilization and period doubling predicted in Langer's self-similar scenario (Langer 1971 *Ann. Phys., NY* **65** 53).

PACS numbers: 05.45.Yv, 47.20.Ky, 47.54.+r

1. Introduction

When a homogenous system suddenly departs from equilibrium, the fluctuations around the initial ground state are linearly amplified and the homogeneous phase can, for example, spontaneously separate into two different more stable states. The interfaces which delimit the numerous resulting monophasic domains will interact with each other, either giving rise to the formation of a complex pattern, or merging into a single interface when the domains of the same state coalesce slowly, minimizing the overall interfacial energy. It then results in only two well-separated domains. This process of first-order phase transition arises particularly for binary mixtures [2], alloys [3] or vapour condensation [4].

It can either initiate via a nucleation process, where the homogeneous state is suddenly put in a metastable configuration and an energy barrier has to be crossed before the transition appears. Or via a spinodal decomposition where the system is led into a linearly unstable configuration. In this latter case, the leading instability selects a modulation of the order parameter at a well-defined length scale, which grows and, due to nonlinearities, saturates. The resulting pattern is composed of well-defined interfaces delimiting domains containing one of the two stable phases. Remarkably, this intermediate stage conserves the modulation width,

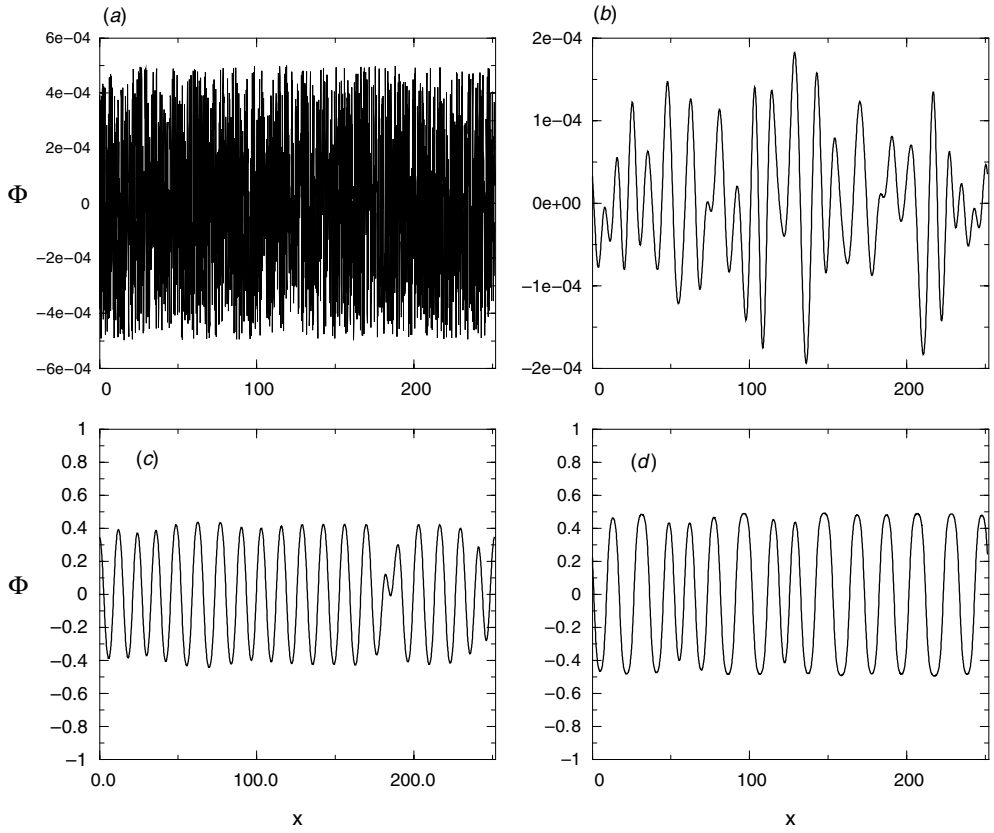

Figure 1. Time evolution of the order parameter $\Phi(x, t)$ for $\varepsilon = -1$, $\mathrm{d}x = 0.1227$: (*a*) initial conditions at $t = 0$ are taken randomly with a very low amplitude (5×10^{-4}); (*b*) at time $t = 15$, the amplitude of the small-scale spatial modulations has been damped by the C–H dynamics, while only long wavelength contributions are still present; (*c*) at $t = 225$, the spatial modulation has almost reached its final amplitude, keeping roughly the same number of peaks as before; (*d*) at $t = 1800$, we observe that the number of domains has decreased from the coarsening dynamics.

and the resulting stationary pattern is of almost the same length scale as the one selected initially [5, 6]. The dynamics finally ends with a much slower, self-inhibiting process, dominated by the interactions between the interfaces. The different regions of each phase coalesce in the so-called Ostwald ripening where the number of domains diminishes whereas their typical size increases. The asymptotic state is decomposed into two domains, one for each phase. In this paper, by spinodal decomposition, we refer to the first stage of the dynamics only, while coarsening will denote the second stage. Although this coarsening dynamics is in fact already present, its influence can often be neglected during the first stage of the process.

Hillert [3], and Cahn and Hilliard [7] have proposed a model equation describing the segregation of a binary mixture. This model, known as the Cahn–Hilliard equation (C–H later on), belongs to the Model B class in Hohenberg and Halperin's classification [8]. It is a standard model for phase transition with conserved quantities and has applications to phase transition in liquid crystals [9], segregation of granular mixtures in a rotating drum [10] or formation of sand ripples [11, 12]. It is a partial differential equation to which a conservative noise is added to account for thermal fluctuations [13].

Figure 1 shows snapshots of a numerical integration of the C–H dynamics which represents the full phase transition process after a quench in temperature. Thermal fluctuations were present in the initial conditions, but have been omitted in the dynamics. The three main stages of the spinodal decomposition described above are clearly distinguished: first, from figures 1(*a*) and (*b*), we observe the selection of a typical length scale for the modulations, and then, from figures 1(*b*) and (*c*), the nonlinear growth and its saturation. We note that the number of peaks has been more or less conserved between these two configurations. In contrast, during the coarsening dynamics observed between figures 1(*c*) and (*d*) the typical length of the pattern increases while, on the other hand, the amplitude of the modulation grows slowly to reach its asymptotic value.

An important activity has been devoted to the description of the dynamics of phase transition, using both statistical methods and numerical simulations (for a review see [14]). The late stage of the spinodal decomposition where the coarsening dynamics dominates exhibits 'dynamical scaling': the dynamics presents a self-similar evolution where time enters only through a length scale $L(t)$, associated with a typical length of the domains or the rate of decay of the inhomogeneities. For instance, scaling arguments and stability criteria give the law $L(t) \sim t^{1/3}$ for spatial dimensions greater than 1 and logarithmic behaviour for one dimension in the case of the C–H equation [14].

This last stage, as observed in the two-dimensional demixion of copolymer [15] and as suggested initially by Langer [1], can be described as a self-similar process of synchronous fusion and evaporation of domains. This observation motivated our work, and the aim of this paper is to present a one-dimensional ansatz describing continuously the coalescence process. This ansatz is in the form of a one-parameter family of symmetric profiles which interpolate between two stationary states composed of homogeneous domains of lengths $\lambda/2$ and λ. It allows us to realize a self-similar sequence of coalescence processes in 1D, starting from the regular micro phase separated states issued from the nonlinear saturation of the spinodal decomposition dynamics and ending with the single interface which characterizes the infinite time, thermodynamic stable state.

The paper is organized as follows: first, we present a brief review on general properties of phase segregations and on the C–H model, mainly to fix the notation. We will reproduce briefly the original derivation by Cahn and Hilliard, restricting ourselves to the one-dimensional case. In section 3, we present a family of symmetric solutions of the Ginzburg–Landau (G–L) equation which is used to study the dynamics of spinodal decomposition and to determine all the symmetric stationary states of the C–H dynamics. Then in section 4, the main original part of this work, we introduce a non-symmetric family of solutions of the G–L equation which is used to construct a continuous interpolation between two consecutive symmetric stationary states. After a study of the energy landscape associated with this ansatz, we finally discuss the numerical accuracy of our calculations. In the conclusion, we justify the hypothesis we have made and compare the suggested scenario with coalescence in real systems.

2. The Cahn–Hilliard model

The Cahn–Hilliard theory is a modified diffusion equation; it is a continuous conservative model for the scalar-order parameter Φ, which reads in its dimensionless form:

$$\frac{\partial \Phi}{\partial t}(\mathbf{r}, t) = \nabla^2 \left(\frac{\varepsilon}{2} \Phi + 2\Phi^3 - \nabla^2 \Phi \right) + \xi(\mathbf{r}, t). \tag{1}$$

The real-order parameter can correspond to the dimensionless magnetization in the Ising ferromagnet, to the fluctuation of the density of a fluid around its mean value during a phase

separation or to the concentration in some region around **r** of one of the components of a binary solution. ε is the dimensionless control parameter of the system; it is often identified with the reduced temperature ($\varepsilon = \frac{T-T_c}{T_c}$, where T_c is the critical temperature of the phase transition). This equation, first derived by Cahn and Hilliard [7], has also been retrieved by Langer [1] from microscopic considerations. As written, the C–H equation does account for thermal fluctuations present in the system through a random white noise $\xi(\mathbf{r}, t)$, whose amplitude is proportional to the square root of the temperature of the system.

The homogeneous stationary solutions for the noiseless C–H equation are extrema of the effective G–L potential $V(\Phi) = \frac{\varepsilon}{2}\Phi^2 + \Phi^4$. For positive ε, there is only one homogeneous solution $\Phi = 0$ which is linearly stable; for negative ε, the stationary solution $\Phi = 0$ undergoes a pitchfork bifurcation and three stationary solutions exist. $\Phi = 0$ is still a stationary solution, but it is now linearly unstable; the two other symmetric solutions $\Phi = \pm\frac{\sqrt{-\varepsilon}}{2}$ are stable and have the same free energy $F = -\varepsilon^2/32$. Thus, a first-order transition can be experienced by suddenly quenching the system from a positive reduced temperature ε to a negative one. Spinodal decomposition is the resulting dynamics.

The stability of the solution $\Phi = 0$ can be studied by linearizing equation (1) around $\Phi = 0$ (i.e., neglecting the nonlinear term Φ^3); considering Φ as a sum of Fourier modes,

$$\Phi(\mathbf{r}, t) = \sum_{\mathbf{q}} \phi_{\mathbf{q}}\, \mathrm{e}^{\mathrm{i}\mathbf{q}\cdot\mathbf{r}+\sigma t} \tag{2}$$

where ϕ_q is the Fourier coefficient at $t = 0$, we obtain for the amplification factor $\sigma(q)$,

$$\sigma(\mathbf{q}) = -\left(q^2 + \frac{\varepsilon}{2}\right) q^2. \tag{3}$$

It immediately shows that $\Phi = 0$ is linearly stable for $\varepsilon > 0$ while a band of Fourier modes is unstable for negative ε, since $\sigma(\mathbf{q}) > 0$ for $0 < q < \sqrt{(-\varepsilon/2)}$. Moreover, the most unstable mode is for $q_{\mathrm{C–H}} = \sqrt{-\varepsilon}/2$ (with $\sigma_{\max} = \frac{\varepsilon^2}{16}$). This wave number of maximum amplification factor will dominate the first stage of the dynamics; in particular, it explains why the modulations appear at length scales close to $\lambda_{\mathrm{C–H}} = 2\pi/q_{\mathrm{C–H}}$, the associated wavelength. Later on, interfaces separating each domain interact through coalescence dynamics, causing $\langle\lambda\rangle$ to change slowly towards higher values [17, 5].

We will now use known results on non-homogeneous solutions of the G–L equation to study both the saturation of the spinodal decomposition and the coalescence.

3. Stationary states of the Cahn–Hilliard dynamics

3.1. Symmetric soliton lattice solutions

For $\varepsilon < 0$, there exists a stationary solution of the one-dimensional C–H equation that relies on the two homogeneous phases $\Phi = \pm\frac{\sqrt{-\varepsilon}}{2}$:

$$\Phi(x) = \frac{\sqrt{|\varepsilon|}}{2} \tanh\left(\frac{\sqrt{|\varepsilon|}x}{2}\right). \tag{4}$$

Such a monotonic solution describes a continuum interface between the two stable homogeneous phases, and corresponds to the thermodynamically stable solution that ends the phase transition dynamics. But this is a particular member of a one-parameter family of stationary solutions of the G–L equation

$$\frac{\varepsilon}{2}\Psi + 2\Psi^3 - \nabla^2\Psi = 0. \tag{5}$$

These solutions, the so-called soliton-lattice solutions, are

$$\Psi_{k,\varepsilon}(x) = k\,\Delta\,\mathrm{Sn}\left(\frac{x}{\xi}, k\right) \qquad \text{with} \quad \xi = \Delta^{-1} = \sqrt{2\frac{k^2+1}{-\varepsilon}} \tag{6}$$

where $\mathrm{Sn}(x, k)$ is the Jacobian elliptic function sine-amplitude, or cnoidal mode. This family of solutions is parametrized by ε^* and by the modulus $k \in [0, 1]$, or 'segregation parameter'. These solutions describe periodic patterns of periods

$$\lambda = 4K(k)\xi \qquad \text{where} \quad K(k) = \int_0^{\frac{\pi}{2}} \frac{\mathrm{d}t}{\sqrt{1-k^2\sin^2 t}} \tag{7}$$

is the complete Jacobian elliptic integral of the first kind. Together with k, it characterizes the segregation, defined as the ratio between the size of the homogeneous domains, $0.5 \times \lambda$, and the width of the interface separating them, $2 \times \xi$. Equation (7) and the relation $\xi = \Delta^{-1}$ enable us to rewrite this family as

$$\Psi_{k,\lambda}(x) = \frac{4K(k)\cdot k}{\lambda}\,\mathrm{Sn}\left(\frac{4K(k)}{\lambda}x, k\right). \tag{8}$$

This family of profiles (or alternating interfaces) can be obtain exactly as a periodic sum of single solitons and antisolitons [18],

$$\sum_n (-1)^n \tanh(\pi s(x-n)) = \frac{2k(s)K(s)}{\pi s}\,\mathrm{Sn}(x, k)$$
$$\text{with} \quad s = \frac{K(k)}{K(k')} \quad \text{and} \quad k'^2 = 1-k^2. \tag{9}$$

3.2. Ansatz for the spinodal decomposition dynamics

The preceding family of profiles can be used to explore the spinodal decomposition dynamics. It can be associated with a micro phase separation, locally limited by the finite diffusion coefficient. For $k = 1$, $\mathrm{Sn}(x, 1) = \tanh(x)$, we recover the usual single interface solution (4) of width $2/\sqrt{|\varepsilon|}$; it is associated with a one soliton solution and corresponds to a strong, or macroscopic segregation. Note that $K(1)$ diverges; the solution

$$\Psi_{1,\varepsilon}(x) = \frac{\sqrt{|\varepsilon|}}{2}\tanh\left(\frac{\sqrt{|\varepsilon|}}{2}x\right) \tag{10}$$

is thus the limit of infinite s, when the solitons, entering in relation (9), are far apart from each other. In the opposite limit (weak segregation regime), it describes a sinusoidal modulation

$$\lim_{k\to 0}\Psi_{k,\varepsilon}(x) = k\sqrt{\frac{|\varepsilon|}{2}}\sin\left(\sqrt{\frac{|\varepsilon|}{2}}x\right) = k\frac{2\pi}{\lambda}\sin\left(\frac{2\pi}{\lambda}x\right) = kq\sin(qx). \tag{11}$$

It will correspond to the Fourier mode $q = \frac{2\pi}{\lambda}$ of the initial white noise, with an arbitrary small amplitude $\nu = kq$. Since experiences, numerical simulations and linear stability analysis show that λ, the spatial period of the pattern, is constant during the whole spinodal decomposition process, we choose λ to coincide with the most unstable wavelength obtained by the Cahn–Hilliard linear approach, $\lambda = \lambda_{\mathrm{C-H}} = \frac{4\pi}{\sqrt{-\varepsilon_0}}$, where ε_0 is the quench temperature. Thus, we obtain a one-parameter family of profiles $\Psi^*(x, k) = \Psi_{k,\lambda_{\mathrm{C-H}}}(x)$ which describes very well both the linear growth and the saturation. The dynamics is now reduced to the time evolution of the single free parameter: $k(t)$. Using equations (6) and (7), we find that λ, k and ε are related to one another through the state equation

$$\varepsilon(k) = -2(1+k^2)\left(\frac{4K(k)}{\lambda}\right)^2. \tag{12}$$

So, this implicit equation tells us that if we fix $\lambda = \lambda_{\mathrm{C–H}}$, the dynamics can also be reduced to the evolution of $\varepsilon(t)$.

Given a periodic function Φ (obtained either from experimental data or numerical simulation of equation (5)) at time t, the ansatz assumes that it corresponds to a soliton lattice of the same period; i.e., there exists $k(t)$ such that $\Psi_{k,\lambda_{\mathrm{C–H}}}(x) \sim \Phi(x,t)$ for each time t. For this purpose, we have developed three different algorithms, taking advantage of the general properties of the family of solutions $\Psi^*(x,k)$: k can be deduced from the amplitude of the oscillation equal to $4kK(k)/\lambda$, from the relation $k = 1 - ((\Psi(\lambda/2,k)/\Psi(\lambda/4,k))^2 - 1)^2$, or from a straightforward computation which relates k to the ratio of the first two Fourier modes of the soliton lattice $\Psi^*(x,k)$. We have observed that the three methods show in general similar results within an error of 1%.

In this approach, $\varepsilon(t)$ can then be interpreted as a fictitious temperature or 'local temperature' of the domains: it is the temperature extracted from the profile at a given time, using the correspondence between ε and k of equation (12). For instance, at $t = 0$, the amplitude is small and we find that $k(0) = \frac{\nu\lambda_m}{2\pi} \to 0$ and thus $\varepsilon^*(0) = 8\pi^2/\lambda^2$, different *a priori* from ε_0 $\left(\varepsilon^*(0) = \frac{\varepsilon_0}{2} \text{ for } \lambda = \lambda_{\mathrm{C–H}}\right)$.

Somehow, the C–H dynamics can be projected at first order onto a dynamics along the sub-family $\Psi^*(x,k) = \Psi_{k,\lambda_{\mathrm{C–H}}}(x)$, which can be considered as an attractor of the solutions, i.e., the density profile of the system will evolve with time, staying always close to a function $\Psi^*(x,k)$. And using a solubility condition, it is possible to compute the full nonlinear part of this dynamics, the saturation of the spinodal decomposition, which leads the system in a well-defined stationary state [6].

3.3. Saturations of the spinodal decomposition dynamics

According to the previous interpretation of the parameter ε, as $\varepsilon(t=0) = \frac{\varepsilon_0}{2}$, the system is initially out of equilibrium. The dynamics will saturate when this fictitious temperature reaches the real thermodynamic one, i.e. the quench temperature ε_0; that is, using equation of state (12) for $\lambda = \lambda_{\mathrm{C–H}}$, when $k = k_0^s$ the solution of the implicit equation,

$$2(1+k_0^{s2})K(k_0^s)^2 = -\frac{\varepsilon_0\lambda_{\mathrm{C–H}}^2}{16} = \pi^2 \qquad \text{that is} \quad k_0^s = 0.687. \tag{13}$$

Note that in this case, the width of the interface, which was initially, just after the quench, proportional to $\frac{2}{\sqrt{-\varepsilon_0}}$, has now become proportional to $\frac{\pi}{\sqrt{-\varepsilon_0}K(k_0^s)} = \frac{\sqrt{2(1+k_0^{s2})}}{\sqrt{-\varepsilon_0}} \backsimeq \frac{1.7}{\sqrt{-\varepsilon_0}}$: the segregation has slightly increased. Using linear stability analysis, Langer has shown that the profile thus obtained, $\Psi^*(x,k_0^s) = \Psi(x,k_0^s,\lambda_{\mathrm{C–H}})$, is destroyed by stochastic thermal fluctuations and he has identified the most unstable mode as an 'antiferro' mode, leading to a period doubling. The result of this destabilization is another profile of an alternate interface, where the length of the domains is now $\lambda = 2\lambda_{\mathrm{C–H}} = \frac{8\pi}{\sqrt{-\varepsilon_0}}$. This means that the new stationary profile is given by $\Psi\left(x,k_1^s,2\lambda_{\mathrm{C–H}}\right)$, where k_1^s is the solution of the implicit relation

$$2\left(1+k_1^{s2}\right)K\left(k_1^s\right)^2 = -\frac{\varepsilon_0(2\lambda_{\mathrm{C–H}})^2}{16} = 4\pi^2 = 8(1+k_0^{s2})K(k_0^s)^2 \qquad \text{that is} \quad k_1^s = 0.985. \tag{14}$$

The interface of this new profile is relatively sharper (the width of the interface is now proportional to $\frac{2\pi}{\sqrt{-\varepsilon_0}K\left(k_1^s\right)} = \frac{\sqrt{2(1+k_1^{s2})}}{\sqrt{-\varepsilon_0}} \backsimeq \frac{2\times 0.99}{\sqrt{-\varepsilon_0}}$) compared to the size of the homogeneous domains which has now doubled, see figure 2. Again, this new stationary profile turns out to be linearly unstable with respect to an 'antiferro' perturbation of period $4\lambda_{\mathrm{C–H}}$.

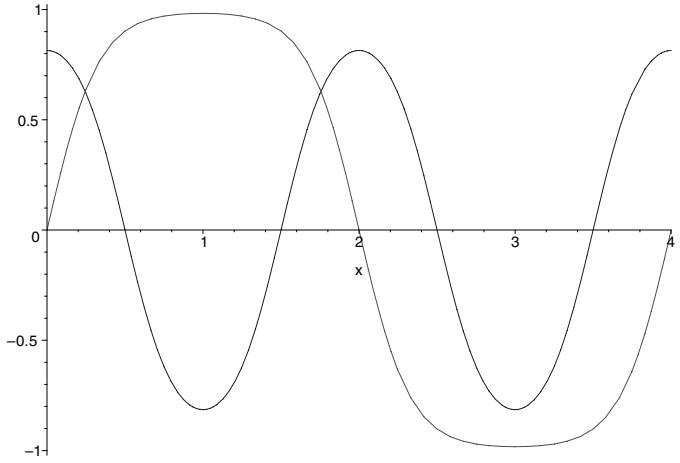

Figure 2. Profiles of the first two metastable solutions of the C–H dynamics, with $k_0^s = 0.687$ and $k_1^s = 0.985$, corresponding to the first coarsening process.

Thus, these families of profiles and instabilities enable us to describe the one-dimensional coarsening as a cascade of doubling processes, leading from a pattern of wavelength $\lambda_{\mathrm{C–H}}$ composed of domains separated by interfaces to a single $\tanh\left(\frac{\sqrt{-\varepsilon_0}}{2}x\right)$ interface separating two semi-infinite domains. Each of these successive intermediate profiles can be described by an element of the above family of soliton lattices $\Psi\left(x, k_n^s, 2^n \times \lambda_{\mathrm{C–H}}\right)$. We thus have a family of segregation parameters $\left\{k_n^s\right\}$, which are determined by the implicit relations

$$2\left(1 + k_n^{s2}\right) K\left(k_n^s\right)^2 = -\frac{\varepsilon_0 (2^n \lambda_{\mathrm{C–H}})^2}{16} = \pi^2 2^{2n}. \tag{15}$$

We have found numerically for the first of them

$k_0^s = 0.686\,979\,5924$	$k_0^s \Delta_0^s = 0.400\sqrt{-\varepsilon_0}$
$k_1^s = 0.985\,167\,5587$	$k_1^s \Delta_1^s = 0.496\,250\sqrt{-\varepsilon_0}$
$k_2^s = 0.999\,972\,101\,65$	$k_2^s \Delta_2^s = 0.499\,990\sqrt{-\varepsilon_0}$
$k_3^s = 0.999\,999\,999\,9027$	$k_3^s \Delta_3^s = 0.499\,998\,46\sqrt{-\varepsilon_0}$

(16)

We see that $\left\{k_n^s\right\}$ converges towards $k_\infty^s = 1$ (single interface case); meanwhile the amplitude of the modulation $k_n^s \Delta_n^s$ goes towards $\sqrt{|\varepsilon_0|}/2$, as can be seen in the second column of equation (16). For large n, we can conclude from the implicit relation (15) that the ratio of the domain size to the interface width characterized by $K\left(k_n^s\right)$ behaves as $\pi 2^{n-1}$. Each of the stationary profiles

$$\Psi_n(x) = \Psi\left(x, k_n^s, 2^n \lambda_{\mathrm{C–H}}\right) = \frac{\sqrt{-\varepsilon_0} K\left(k_n^s\right) \cdot k_n^s}{2^n \pi} \operatorname{Sn}\left(\frac{\sqrt{-\varepsilon_0} K\left(k_n^s\right)}{2^n \pi} x, k_n^s\right), \tag{17}$$

for which the interface width is proportional to $\frac{2^n \pi}{\sqrt{-\varepsilon_0} K\left(k_n^s\right)}$ (which tends to $\frac{2}{\sqrt{-\varepsilon_0}}$, in agreement with $\tanh\left(\frac{\sqrt{-\varepsilon_0}}{2}x\right)$), is identically destroyed by the Langer 'antiferro' instability.

4. An ansatz for the 1D coarsening process

4.1. Non-symmetric soliton lattice profile

In order to describe one step of the coalescence process, i.e., the dynamics that starts from $\Psi_n(x)$ and ends with the profile $\Psi_{n+1}(x)$, we will use another family of equilibrium profiles [19], solutions of the G–L equation, which can be written as

$$\psi(a,k,x) = \frac{\alpha(a,k) - k/\sqrt{a}\,\beta(a,k)\,\mathrm{Sn}\big(4x\frac{K(k)}{\lambda},k\big)}{1 - k/\sqrt{a}\,\mathrm{Sn}\big(4x\frac{K(k)}{\lambda},k\big)} \tag{18}$$

where

$$\alpha(a,k) = \frac{-2k^2/a + 1 + k^2}{((1+k^2)^2 - 12k^2 + 2(a+k^2/a)(1+k^2))^{\frac{1}{2}}}$$

and

$$\beta(a,k) = \frac{2a - 1 - k^2}{((1+k^2)^2 - 12k^2 + 2(a+k^2/a)(1+k^2))^{\frac{1}{2}}}.$$

It is still a periodic lattice of interfaces, but now, the mean value of the order parameter is nonzero (non-symmetric case). It is controlled by the parameter $a \geqslant 1$: if a goes to infinity, we recover the previous family of periodic profiles.

4.2. Ansatz for the continuous interpolation between two stationary states

If we choose a to be equal to $1 + k'$ (where $k'^2 = 1 - k^2$), we can then construct symmetric profiles using the sum of two non-symmetric ones. Indeed, using Gauss' transformation (or descending Landen transformation [20]), which relates the soliton lattice of spatial period 2λ (and of modulus k) to the soliton lattice of period λ (and of modulus $\mu = \frac{1-k'}{1+k'}$), we have

$$1 - \frac{\sqrt{5-k^2}}{2}\left(\psi\left(k, x - \frac{\lambda}{2}\right) + \psi\left(k, x + \frac{\lambda}{2}\right)\right) = k\,\mathrm{Sn}\left(2x\frac{K(k)}{\lambda}, k\right) \tag{19}$$

$$1 - \frac{\sqrt{5-k^2}}{2}(\psi(k, x-\lambda) + \psi(k, x+\lambda)) = (1-k')\,\mathrm{Sn}\left((4x+2\lambda)\frac{K(\mu)}{\lambda}, \mu\right) \tag{20}$$

where $\psi(k,x) = \psi(1+k', k, x)$. Thus, we then can show from equation (19) that

$$K(k)\left[1 - \frac{\sqrt{5-k^2}}{2}\left(\psi\left(k, x - \frac{\lambda}{2}\right) + \psi\left(k, x + \frac{\lambda}{2}\right)\right)\right] = kK(k)\,\mathrm{Sn}\left(2x\frac{K(k)}{\lambda}, k\right). \tag{21}$$

This is the solution of the G–L equation of period 2λ. Moreover, if we use the fact that

$$K(k) = \frac{2}{1+k'}K(\mu) \qquad \text{or} \qquad K(\mu) = \frac{1}{1+\mu}K(k) \tag{22}$$

we can write

$$(1-k')K(k)\,\mathrm{Sn}\left((4x+2\lambda)\frac{K(\mu)}{\lambda}, \mu\right) = 2\mu K(\mu)\,\mathrm{Sn}\left((2x+\lambda)\frac{2K(\mu)}{\lambda}, \mu\right). \tag{23}$$

Then, using relation (20), the solution of the G–L equation of period λ can be expressed as

$$K(k)\left[1 - \frac{\sqrt{5-k^2}}{2}(\psi(k, x-\lambda) + \psi(k, x+\lambda))\right] = 2\mu K(\mu)\,\mathrm{Sn}\left((2x+\lambda)\frac{2K(\mu)}{\lambda}, \mu\right). \tag{24}$$

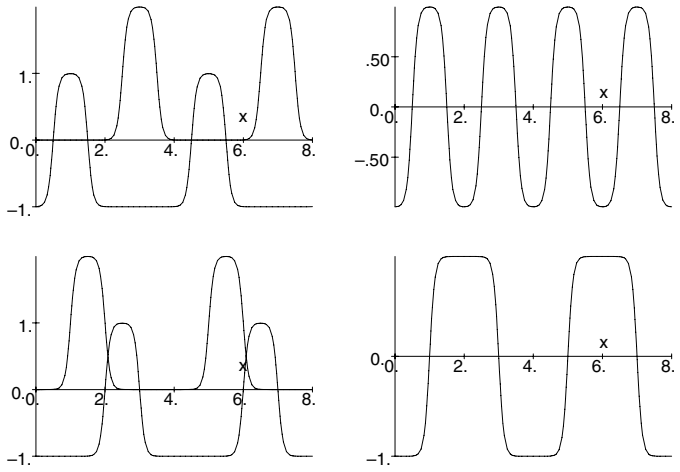

Figure 3. Construction of the first two steady solutions of the C–H dynamics, with $k_0^s = 0.687$ and $k_1^s = 0.985$, using a superposition of the non-symmetric profile $\psi(k, x)$, which itself is a stationary solution of the C–H equation. By changing the phase shift between the two profiles entering into the linear combination, one obtains two different symmetric profiles, of periods λ and 2λ.

So, we see that both the initial state $\Psi^*\left(x, k_{n-1}^s, 2^{n-1}\lambda_{\mathrm{C–H}}\right)$ and the final state $\Psi^*\left(x, k_n^s, 2^n\lambda_{\mathrm{C–H}}\right)$ of a step of the coalescence process can be described, modulo a phase shift, by the same function:

$$\Phi(x, k, \phi) = \frac{4K(k)}{\lambda}\left[1 - \frac{\sqrt{5-k^2}}{2}(\psi(k, x - (1-\phi/2)\lambda) + \psi(k, x + (1-\phi/2)\lambda))\right] \quad (25)$$

with $k = k_n^s$ and $\lambda = 2^n\lambda_{\mathrm{C–H}}$. Therefore, we can describe the coalescence by a transformation at a constant segregation parameter k, while the degree of freedom ϕ, associated with the relative phase between the two profiles, evolves in time from 0 to 1 according to the C–H dynamics.

This non-symmetric lattice of interfaces can be interpreted as a periodic sum of alternating single interfaces (kinks and antikinks). In the same spirit as relation (9), if one forgets in the infinite sum every two out of four interfaces, one gets

$$\psi(x) \sim \sum_p [\tanh(\pi s(x - 4 * p)) - \tanh(\pi s(x - 4 * p + 1))]. \quad (26)$$

Then (see figure 3) adding $\psi(x + 2)$ to $\psi(x)$ enables us to recover relation (9), while, after a translation, adding $\psi(x + 1)$ and $\psi(x)$ gives the soliton lattice of double period, because of the cancellation of half of the interfaces (annihilation of kinks and antikinks).

If we look at the time evolution of the profile $\Phi(x, k, \phi)$, starting from the region $\phi = 0$, we can transform the C–H equation into a phase field equation, replacing $\frac{\partial}{\partial t}\Phi(x, k, \phi)$ by $\frac{\partial}{\partial \phi}\Phi(x, k, \phi(t))\frac{\mathrm{d}\phi}{\mathrm{d}t}$. The dynamics will be similar to a spinodal decomposition, with ϕ growing and saturating exponentially. $\frac{\partial}{\partial \phi}\Phi(x, k, \phi)$ is the most unstable mode founded in Langer's linear stability analysis, characterized by the alternate growth and decrease of domains ('antiferro' mode). Note that when Langer was studying the most unstable perturbation, he was looking at the linearized version of the C–H equation around $\Psi^*(k, x) = \Psi(x, k, \lambda_{\mathrm{C–H}})$:

$$\mathcal{L}\varphi = \left(\frac{\varepsilon}{2} + 6\Psi^{*2} - \nabla^2\right)\varphi = \left(\frac{\varepsilon}{2} + n \times (n+1)\Psi^{*2} - \nabla^2\right)\varphi. \quad (27)$$

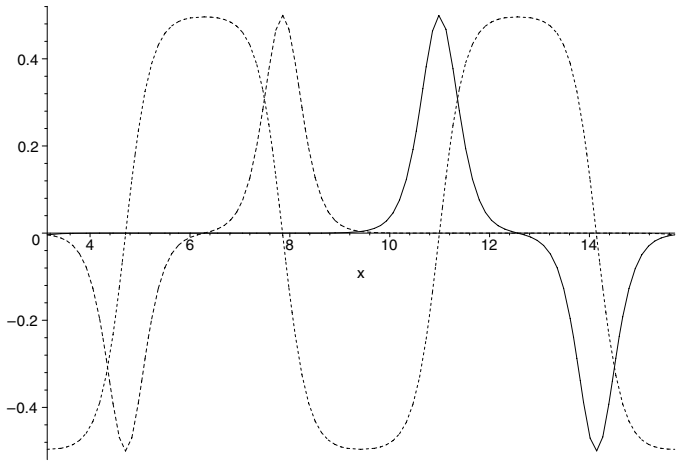

Figure 4. Langer's most unstable perturbation mode of destabilization of the soliton lattice is identified with $\frac{\partial}{\partial\phi}\Phi(x,k,\phi)$ at $\phi=0$. It is composed of two antisymmetric patterns, plotted with a dotted (solid) line, evolving towards the right (left) at velocity $+\frac{\mathrm{d}\phi}{\mathrm{d}t}$ $(-\frac{\mathrm{d}\phi}{\mathrm{d}t})$, causing an 'antiferro' instability leading to a period doubling of the pattern. They are the spatial derivatives of the initial non-symmetric profile $\psi(x)$ which have been used to construct our ansatz in figure 3.

$\mathcal{L}\varphi = E\varphi$ is the Lamé equation, for $n=2$ (here $\varepsilon_0=1$). This equation does not have a simple (algebraic) exact eigenfunction of period $2\lambda_{\mathrm{C-H}}$ [21]. $\frac{\partial}{\partial\phi}\Phi(x,k,\phi)$ for $\phi=0$ is not an exact eigenfunction either[1]. Nevertheless, it happens to be a good approximation for the eigenfunction of the lowest eigenvalue. Due to the concavity of $\mathcal{F}(\phi)$ around $\phi=0$ (see figure 5), this eingenvalue will be negative, triggering a linear destabilization and an exponential amplification of the perturbation, i.e. an exponential growth of the translation ϕ with time.

Langer's phenomenon of 'antiferro' instability appears due to the existence of two possible directions for the displacement of the interfaces 'tanh' (or of the non-symmetric lattice of interfaces ψ), one with a positive velocity $\left(+\frac{\mathrm{d}\phi}{\mathrm{d}t}\right)$ and one with a negative one $\left(-\frac{\mathrm{d}\phi}{\mathrm{d}t}\right)$. The four different kinds of interfaces present in a cell of length $2\lambda_{\mathrm{C-H}}$ have alternately a positive or a negative velocity. This can be seen as the existence of two antisymmetric patterns [22], or building blocks for the leading instability around an intermediate state $\Psi^*\left(x, k_n^s, 2^{n-1}\times\lambda_{\mathrm{C-H}}\right)$ (see figure 4). The two building blocks, $\pm\frac{\mathrm{d}}{\mathrm{d}x}\psi(x)$, are associated with the two pairs of interfaces, $\psi(x)$ and $\psi(x+2)$, which have been used to construct our ansatz.

Note that in Langer's analysis, the breaking of symmetry for the choice of the antiferro cell corresponds here to the freedom we have when choosing the range of variation of ϕ: we could have chosen to go from 0 to -1, ending after a step of coarsening with the symmetric pattern (a pattern translated of half a period).

4.3. Energy landscape

In order to prove the usefulness of this ansatz, we have plotted the energy averaged over the final period, $\mathcal{F}(\phi)=\int F(\Phi(x,k,\phi))\,\mathrm{d}x$, as a function of the parameter ϕ, keeping k constant.

[1] $\frac{\partial}{\partial\phi}\Phi(x,k,\phi=0)$ corresponds to a local maximum of the free energy averaged over one period $\mathcal{F}(\phi)=\int F(\Phi(x,k,\phi))\,\mathrm{d}x$. The G–L or stationary C–H equation, i.e. the first functional derivative $\frac{\delta F}{\delta\Phi}=0$, admits $\Phi(x,k,\phi=0)=\Psi^*(x)$ as a solution. But the Lamé equation, obtained when linearizing the G–L equation around $\Psi^*(x)$, is related to the second functional derivative of F; therefore, one does not expect $\frac{\partial}{\partial\phi}\Phi(x,k,\phi=0)$ to be an exact solution or eigenfunction of $\mathcal{L}$.

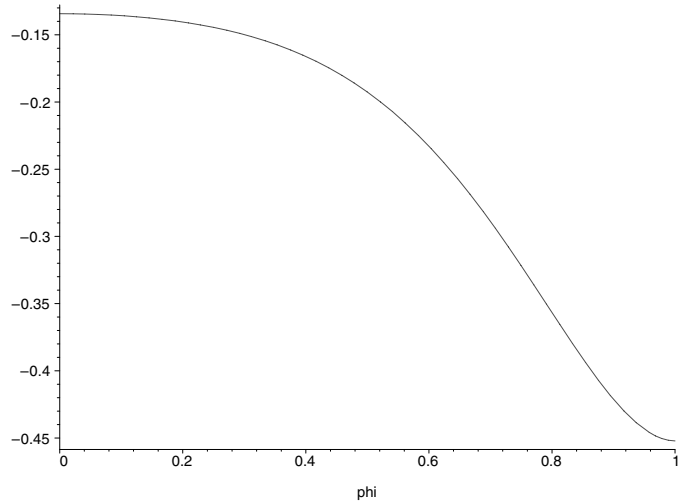

Figure 5. Profile of the free-energy landscape during a coarsening process, $F(\phi)$. It starts at $\phi = 0$ for a configuration characterized by the segregation ratio $k_0^s = 0.687$ for which the energy per unit length is $F(\phi = 0) \simeq -0.135$; one sees that in this region, the free energy is a concave function of ϕ and thus the associated pattern is linearly unstable. The elementary step of the coarsening process ends for $\phi = 1$ associated with a pattern characterized by the segregation ratio $k_1^s = 0.985$ for which the energy per unit length is $F(\phi = 1) \simeq -0.45$. In the region $\phi = 1$, the free energy is a convex function of ϕ.

We see, for example, in figure 5 that the value $\phi = 0$ corresponds to a local maximum of energy, while $\phi = 1$ (or -1) is a minimum. Note that there is no energy barrier in this particular energy landscape, in agreement with the linear stability analysis.

4.4. Approximation for adiabatic evolution with constant k

Relation (15) enables us to write an implicit relation between k_n and k_{n+1}:

$$\sqrt{1 + k_{n+1}^{s2}}\, K\left(k_{n+1}^s\right) = 2\sqrt{1 + k_n^{s2}}\, K\left(k_n^s\right). \tag{28}$$

It is in fact different from relation (22) obtained by the Landen transformation. Nevertheless in the region $k \geqslant k_0^s = 0.687$, the two transformations almost coincide, as can be seen in figure 6. As this is especially true close to $k = 1$, and as this region is rapidly reached after the second or third iteration, we pretend that the process of coarsening can be described with reasonable accuracy by our ansatz at constant k. A slight change in segregation parameters during the nth doubling process, from $k = \mathrm{Landen}\left(k_n^s\right)$ when $\phi = 0$ to $k = k_{n+1}^s$ when $\phi = 1$, is present in the dynamics, as seen in equation (29):

$k_0^s = 0.686\,979\,5924$	$\mathrm{Landen}^{-1}\left(k_1^s\right) = \mathrm{Gauss}\left(k_1^s\right) = 0.707\,074\,3852$
$\mathrm{Landen}\left(k_0^s\right) = 0.982\,634\,6738$	$k_1^s = 0.985\,167\,5587$
$\mathrm{Landen}\left(k_1^s\right) = 0.999\,972\,0868$	$k_2^s = 0.999\,972\,101\,65$
$\mathrm{Landen}\left(k_2^s\right) = 0.999\,999\,9998$	$k_3^s = 0.999\,999\,999\,902\,745$

(29)

But it has only a minor effect in terms of the profile shape $\Phi(x, k, \phi)$. This means that the dynamics of the parameter k, which affects the value of the modulus by 0.25% during the first

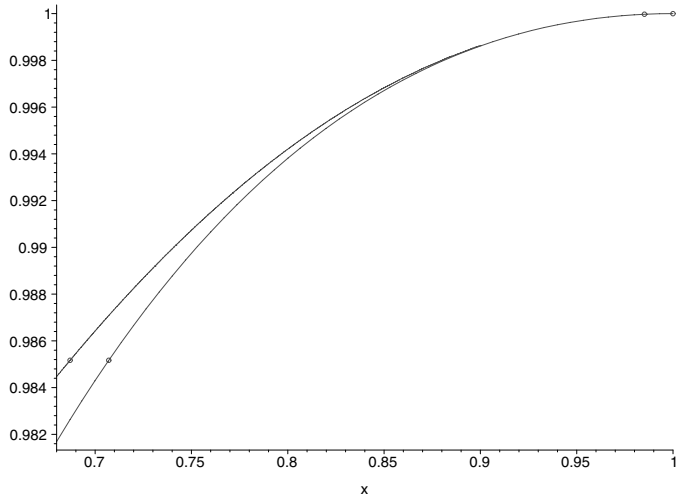

Figure 6. Comparison between the Landen transformation (upper solid line) and the implicit relation between consecutive stationary steady states of the C–H equation $(1 + k_{n+1}^2)^{\frac{1}{2}} K(k_{n+1}) = 2(1 + k_n^2)^{\frac{1}{2}} K(k_n)$ (lower dashed line) in the region between $k = k_0^s = 0.68$ and $k = 1$, corresponding to the region of interest for the coarsening process. The Landen transformation relates the segregation parameter of a soliton lattice of period λ to the segregation parameter associated with a lattice of period 2λ. It is the generalization for the cnoidal function of the usual relation $\sin 2\theta = 2 \sin\theta \cos\theta$. The circles mark (from left to right) k_0^s, Landen$^{-1}(k_1^s)$, k_1^s and Landen$^{-1}(k_2^s)$. If the doubling process associated with the coarsening were only a phase shift of ϕ between 0 and 1, the two curves would have coincided, i.e., the implicit relation (28) would be equivalent to the Landen transformation. As it is not the case, there is a k change during the doubling process, but only of a few per cent, as can be seen numerically in equation (29). Moreover, one sees that, as the coarsening process takes place, k reaches values more and more close to 1 for which the disagreement becomes negligible: the k change becomes increasingly smaller.

step of coarsening, becomes negligible as k goes closer to 1. So we can conclude that this 'k-dynamics' is irrelevant; this parameter can be considered as constant during the evolution of ϕ.

5. Discussion on the hypothesis

Our analytical method relies on the assumption that at each step of the dynamics, the system can be characterized by a specific spatial period: we therefore need to discuss how this approach is relevant to the general case where noise is present. We have numerically noted that, for the spinodal decomposition, the average size of the modulation is λ_{C-H}, with a deviation of less than 1% from the value predicted by the linear theory. It does not mean that, in a real system, each domain has a length scale of λ_{C-H}, but that the distribution of the lengths of the domains will be centred around λ_{C-H} [6]. The coalescence events, due to initial fluctuations in the periodicity of the pattern selected just after the quench, can be neglected during the initial growth of the amplitude of the modulation. Only after this initial growth has saturated (as can be seen in figure 1), does the coalescence process start, which will then dominate the dynamics: the typical length scale of the structures increases slowly with time.

As suggested in [1, 15], we can suppose that during the ideal coalescence process, each lattice of interfaces will experience an antiferro instability. By an ideal coalescence, we mean a process which breaks as few symmetries as possible. But in a real system, this instability

will concern a region of finite size, where it chooses a certain sublattice, or a range for ϕ (for example, ϕ varies from 0 to 1), while it is the opposite choice in the neighbouring region (ϕ varies from 0 to -1). Thus overall, the global symmetry is recovered. During each step of the process, the width of the domains will locally double. But due to non-synchronization between the regions, for the system as a whole, the average length scale will vary continuously.

Acknowledgment

The author is indebted to Christophe Josserand for many fruitful discussions and comments together with numerical help.

References

[1] Langer J S 1971 *Ann. Phys., NY* **65** 53
[2] Wagner C 1961 *Z. Electrochem.* **65** 581
[3] Hillert M 1961 *Acta Metall.* **9** 525
[4] Langer J S 1992 *Solids Far from Equilibrium* ed C Godrèche (Cambridge: Cambridge University Press) pp 297–363
[5] Izumitani T and Hashimoto T 1985 *J. Chem. Phys.* **83** 3694
[6] Villain-Guillot S and Josserand C 2002 *Phys. Rev.* E **66** 036308
[7] Cahn J W and Hilliard J E 1958 *J. Chem. Phys.* **28** 258
[8] Hohenberg P C and Halperin B I 1977 *Rev. Mod. Phys.* **49** 435
See also Cross M C and Hohenberg P C 1993 *Rev. Mod. Phys.* **65** 851
[9] Chevallard C, Clerc M, Coullet P and Gilli J M 2000 *Eur. Phys. J.* E **1** 179
[10] Oyama Y 1939 *Bull. Inst. Phys. Chem. Res. Rep.* **5** 600
Puri S and Hayakawa H 2001 *Adv. Complex Syst.* **4** 469–79 (*Preprint* cond-mat/9901260)
[11] Scherer M A, Melo F and Marder M 1999 *Phys. Fluids* **11** 58
[12] Stegner A and Wesfreid J E 1999 *Phys. Rev.* E **60** R3487
[13] Cook H E 1970 *Acta Metall.* **18** 297
[14] Lifshitz I M and Slyozov V V 1961 *J. Phys. Chem. Solids* **19** 35
Bray A J 1994 *Adv. Phys.* **43** 357
[15] Joly S, Raquois A, Paris F, Hamdoun B, Auvray L, Ausserre D and Gallot Y 1996 *Phys. Rev. Lett.* **77** 4394
[16] Gunton J D, San Miguel M and Sahni P S 1983 *Phase Transitions and Critical Phenomena* vol 8, ed C Domb and J L Lebowitz (London: Academic) p 267
[17] Langer J S, Bar-on M and Miller H D 1975 *Phys. Rev.* A **11** 1417
[18] Saxena A and Bishop A R 1991 *Phys. Rev.* A **44** R2251
[19] Novik-Cohen A and Segel L A 1984 *Physica* D **10** 277
[20] Abramowitz M and Stegun I 1965 *Handbook of Mathematical Functions* (New York: Dover)
[21] Arscott F M 1981 *Periodic Differential Equations* (Oxford: Pergamon)
[22] Coullet P, Goldstein R E and Gunaratne J H 1989 *Phys. Rev. Lett.* J. **63** 1954